

A. WOŹNIAK<sup>1</sup>, O. BIALAS<sup>1</sup>, M. ADAMIAK<sup>1\*</sup>

## IMPROVEMENT OF THE PROPERTIES OF Ti6Al7Nb TITANIUM ALLOY IN TERMS OF THE TYPE OF SURFACE MODIFICATION

The paper presents the influence of ZrO<sub>2</sub> coating on Ti6Al7Nb titanium alloy depending on the method of deposition. The coatings were made by sol-gel method and atomic layer deposition (ALD). Wettability tests, pitting corrosion assessment and electrochemical impedance spectroscopy (EIS) were carried out in the paper. Complementary macro- and microscopic observations, roughness analysis by profilometric method and atomic force microscopy (AFM) were made. Based on the results obtained, it can be concluded that the type of method of depositing the layer on the surface of the material has a significant influence on its properties and that it should be taken into account during the process of the material improvement. Drawing on the findings presented, it can be inferred that roughness has a significant impact upon the surface wettability of the tested surfaces and their related corrosion resistance. The obtainment of hydrophobic surfaces is for smaller roughness values.

*Keywords:* titanium alloys; sol-gel method; ZrO<sub>2</sub> coating; EIS; AFM

### 1. Introduction

Constantly increasing estimated human life expectancy leads to a dramatic increase in orthopaedic interventions due to wear and tear of natural, sensitive biomechanical elements of the skeletal system [2,12,18]. For this reason and in order to continuously improve the properties of implanted materials in the human body, new materials require special supplies. Speaking of metallic biomedical materials and their application in trauma surgery or orthopedics, it is impossible not to distinguish titanium as the most widely used material in medicine to reconstruct lost biomechanical functions [6-8,16].

Titanium in view of its specific properties, meet the biocompatibility criteria set for it in a way unattainable for other materials. Among them, the following should be noted in particular all high corrosion resistance in the tissue environment, low density with appropriate mechanical properties, low tribological wear, paramagnetic properties, low electrical and thermal conductivity and inertness in the biological environment. Additionally, the possibility of lowering the longitudinal modulus of elasticity (Young's module) is of great importance for implants that are compatible with bone. Direct structural and functional connection between the ordered, live bone and the surface of the loaded

implant is so called osseointegration which is possible due to all factors above [5,9-11,13-15,19].

In order to increase the applicability of titanium and its alloys, numerous surface modification methods are used. One of them is the application of a thin layer of zirconium oxide. The multitude of variants of the methods of coatings deposition on the surface of materials raises the need to answer the question which method is the most advantageous.

Reports in the literature suggest that the surface alteration of titanium by sol-gel process deposition on their surface thin oxide layers has a significant effect on the enhancement of this material's properties. The sol-gel process is typically used to apply single- and multi-component and multi-layer coating. The oxide layer deposited in this process is distinguished by a different chemical composition and microstructure that exceeds the value of 1 μm in thickness. In addition, one of the benefits of the sol-gel process is the possibility of creating hydroxyapatite directly on the accumulated surfaces due to the contact with the physiological liquid. The surface of ZrO<sub>2</sub>, whose oxides are present in three crystallographic variants, the most advantageous of which is high temperature one, because of its better mechanical properties, which are measured by high hardness, good bending strength and elasticity in cracking. In addition,

<sup>1</sup> SILESIAN UNIVERSITY OF TECHNOLOGY, FACULTY OF MECHANICAL ENGINEERING, DEPARTMENT OF ENGINEERING MATERIALS AND BIOMATERIALS, 18 A KONARSKIEGO STR., 44-100, GLIWICE, POLAND

\* Corresponding author: marcin.adamiak@polsl.pl



it has very good anticorrosive properties, which translates into high biocompatibility [1,4,17].

The second method of deposition of coatings on the surface of material, compared in this article, is the atomic layer deposition (ALD) method belonging to the family of Chemical vapour deposition (CVD) techniques. The CVD is a process in which films of materials are deposited on the surface of a substrate by decomposition of chemicals from the vapor phase. The process is most often thermally guided but also photo- and plasma-assisted methods are used. Film deposition is controlled through a chemical reaction. Hence the method is more versatile than many of the traditional methods. Growth is under conditions of nonequilibrium, and the nature of the chemical precursor can be used in principle to control the deposited phase and its morphology. Other benefits of the method include a potential for both conformal and large-scale growth, and the possibility of achieving very high levels of reproduction [3,20]. The aim of this paper is to identify a more favorable variant of the method of depositing on the properties of the coating.

## 2. Materials and methods

The investigated material was titanium alloy Ti-6Al7Nb (Forecreu S.A) in form of disc of diameter  $\phi = 14$  mm and thickness  $d = 4$  mm. The chemical composition of the tested material met the requirements of the PN-EN ISO 5832-11 and was presented in Table 1.

TABLE 1  
Chemical composition of Ti6Al7Nb alloy [22]

Elements, [%]	Certificate	ISO 5832-11
Al	5.70	6.00
Nb	6.70	7.00
Ta	0.44	>1.20
Fe	0.18	>0.20
O	0.16	>0.18
C	0.04	>0.05
N	0.02	>0.04
H	0.007	>0.008
Ti	rest	rest

The tested samples were subjected to mechanical treatment, which consisted of two consecutive processes: mechanical grinding, which was performed using abrasive SiC paper with the grain density of 220, 800, 1200 and 2400 grain/mm<sup>2</sup> and mechanical polishing, which was carried out with standard colloidal silica suspension – OP-U 0.04  $\mu\text{m}$ . The mechanical finishing processes were performed with the use of grinding-polishing machine TERGAMIN – 30 by Struers. In the next steps the samples were divided into two group depending of the type of the surface modification method – first by sol-gel method, second by the ALD method. The zirconia oxide layer  $\text{ZrO}_2$  were deposited on the surface of the samples.

The colloidal solution of zirconia oxide was prepared by mixing zirconium isopropoxide  $\text{Zr}(\text{OC}_3\text{H}_7)_4$  as a zirconia oxide

precursor with 2-propanol in the presence of acetylacetonate  $\text{C}_5\text{H}_8\text{O}_2$  as an inhibitor and yttrium nitrate  $\text{Y}(\text{NO}_3)_3 \times 6\text{H}_2\text{O}$  as a yttrium precursor. The reaction substrates were infused in several stages (Fig. 1) and each time terminating with thorough mixing of the solution. The mixing were performed with speed of 300-600 rpm with the use of magnetic stirrer CAT EXM 6 (Germany). The sol-gel process was performed in the protective atmosphere of nitrogen. At the final stage of the gel preparation, the distilled water and 2-propanol were dosed to the solution using the “drop by drop” method, until a homogeneous gel of modified zirconium oxide 98%  $\text{ZrO}_2 + 2\% \text{Y}_2\text{O}_3$  was obtained (Fig. 1). The obtained gel were deposited on tested samples by a single dip coating process at a constant withdrawal speed. In the next stage the samples with the oxide layer were subjected to the heat treatment at Renfert Magma furnace. The samples were baked at an initial temperature  $T = 50^\circ\text{C}$  for time  $t = 60$  min and next the temperature was increased to  $T = 100^\circ\text{C}$  and the samples were baked for  $t = 120$  minute (the heating rate was equal to  $V = 5^\circ\text{C}/\text{min}$ ).

The surface of second samples group was modified by the Atomic Layer Deposition ALD. A zirconia oxide layer was deposited on the tested samples using TFS – 200 – 190 reactor by Beneq. TEMAZr (Tetrakis(ethylmethylamido) zirconium(IV)) was used as a precursor for zirconia. The process was carried out in nitrogen atmosphere. Growth per cycle (GPC) for  $\text{ZrO}_2$  (at the ALD process temperature of  $200^\circ\text{C}$ ) was approximately 0.092 nm/cycle.

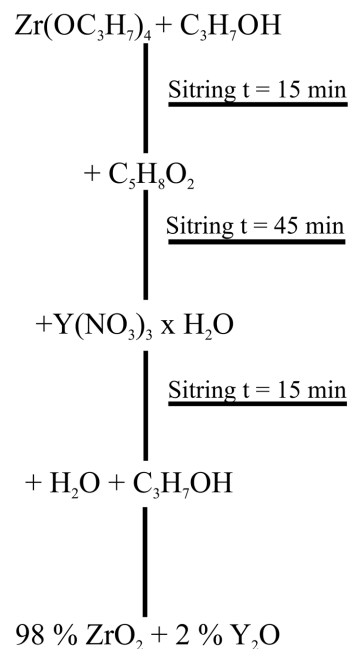


Fig. 1. Sol-gel method steps

### 2.1. Macroscopic observation

Macroscopic measurements of the surfaces were carried out using the stereomicroscope SteREO Discovery by ZEISS. Macroscopic observations were carried out before and after pitting corrosion test.

## 2.2. AFM analysis

In the next step, microscopic observation was performed with the use of Atomic Force Microscopy to obtain additional information on surface topography of the tested specimens. The study was performed using a non-contact mode using the Park System XE-100 microscope. The parameter describing the roughness of the layer – the arithmetic average of the profile of ordinates ( $R_a$ ) was measured over a scan area of  $25 \times 25 \mu\text{m}$ .

## 2.3. Surface roughness analysis by profilometric method

Measurements of surface roughness were carried out using the touch method with a Surftronic 25 surface roughness tester by Taylor Hobson (Poland). The size of the measurements was 0.8 mm and the accuracy of the measurements was  $\pm 0.1$  mm. Roughness parameter  $R_a$  – arithmetic mean value of roughness calculated the measurement results obtained. An average of five measurements were given on each specimen.

## 2.4. Contact angle measurements and Surface Free Energy Calculation

Measurements of the touch angle are carried out to assess the physicochemical properties. The study was conducted using a test stand, which included OGE's Surftronic Universal goniometer (OEG Company, German) and a Surface 4.5 computer PC for analysis of the reported fall image. Drops of the measured liquids – distilled water (POCH S.A, Poland) and diiodomethane (Merck, Poland) are mounted on the surface of the test samples, each with a volume of  $1.5 \mu\text{l}$ . The experiments were carried out at room temperature  $T = 23 \text{ }^\circ\text{C}$  and started 20 s after the sample drops had been dispensed. The surface-free energy (SFE) values for the Owens-Wendt method and their polar and dispersion properties are given in Table 2.

TABLE 2

The values of SFE and their polar and apolar components for measure liquids used in Owens – Wendt method [22,23]

	Measure Liquids	
	Distilled water	Diiodomethane
$\gamma_L$ , [mJ/m <sup>2</sup> ]	72.80	50.80
$\gamma_L^d$ , [mJ/m <sup>2</sup> ]	21.80	0.00
$\gamma_L^p$ , [mJ/m <sup>2</sup> ]	51.00	0.00

## 2.5. Potentiodynamic test

In the next step, the potentialodynamic tests were performed by recording the anodic polarization curves to evaluate the resistance to pitting corrosion. To this end, a VoltaLAB PGP201

potentiostat, a device with VoltaMaster 4 software and an electrochemical cell similar to the one used in the potentialodynamic experiment were included in the test stand. From the initial potential  $E_{int} = E_{ocp} - 100$  mV, the anodic polarization curves were reported. The potential change was at a speed of 1 mV/s in the direction of the anodic. Once the anodic current density has reached  $I = 1$  mA/cm<sup>2</sup> or the potential has reached  $E = 4000$  mV, the direction of polarization has changed and the return curves have been registered. The values of the characteristic parameter of the pitting corrosion resistance are calculated on the basis of the reported curves:  $E_{corr}$  [mV] corrosion potential,  $E_{tr}$  [mV] transpassivation potential,  $R_p$  [k·cm<sup>2</sup>] polarization resistance. The current density of corrosion was determined from the  $i_{corr} = 0.026/R_p$  equation. Research was conducted at temperature  $T = 37 \pm 1$  °C in 250 ml Ringer solution (pH =  $6.9 \pm 0.2$ ). Table 3 shows the chemical composition of the used Ringer solution.

TABLE 3

Chemical compositions of the used Ringer solution

Compound	Concentration, [g/l]
Sodium chloride	8.60
Potassium chloride	0.30
Calcium chloride dehydrate	0.33

## 2.6. Electrochemical Impedance Spectroscopy test

The study of Electrochemical Impedance Spectroscopy (EIS) was performed to determine the physicochemical properties of the examined samples. The study was conducted using the PGSTAT 302N (nLAB, POLAND) measuring system of AutoLab fitted with the FRA2 unit Frequency Response Analyzer and the three-electrode electrochemical cell: working electrode (anode), test sample, auxiliary electrode, platinum wire (PTP-201) and reference electrode – calomel electrode (SECKP-113). The system allowed testing in the frequency range of  $10^4$ - $10^{-3}$  Hz and the voltage amplitude of sinusoidal signal actuating was 10 mV. The impedance device spectra are calculated in the form of Nyquist diagrams and Bodes diagrams on the basis of the taken sample. The measurement data obtained have been adapted to the replacement setup using the method of the smallest squares and the values of resistance  $R$  and capability  $C$  have been calculated. The EIS test in the same conditions as the potentiodynamic polarization test experiment was performed.

## 3. Results

### 3.1. Microscopic observation

The microscopes observation of the tested samples are presented in Figure 2. The structures of the samples in initial state and after surface modification, regardless of the type of using method were homogenous. For the both samples group with zirconia oxide layer  $\text{ZrO}_2$  were characterized by defect



Fig. 2. Results of macro- and microscopic observation a) Ti<sub>is</sub>, b) Ti<sub>sg</sub>, c) Ti<sub>ald</sub>



Fig. 3. Results of microscopic observation of a) Ti<sub>is</sub>, b) Ti<sub>sg</sub>, c) Ti<sub>ald</sub>, after pitting corrosion tests

free surface morphology – the deposited layers were uniform, with no spalling and discoloration. The surface topography of tested samples before and after pitting corrosion test were similar (Fig. 3).

### 3.2. AFM analysis

The results of Atomic Force Microscopy in the form of 3D maps of surface topography for all tested samples are presented in Figure 4. Based on this it can be concluded that the type of

surface treatment has significantly affected on the quality of surface topography. The samples in the initial state Ti<sub>is</sub> were characterized by a larger surface development in comparison to samples with the ZrO<sub>2</sub> layer (Fig. 4a). Deposited layer regardless of the modified method was very thin – in case of sol-gel method thickness of the obtained layers were less than 130 nm and in case of ALD method was an approximately 50 nm, therefore the layers reproduce the topography of the samples in the initial state. However, the surface with zirconia oxide layer were characterized by defect free structure.

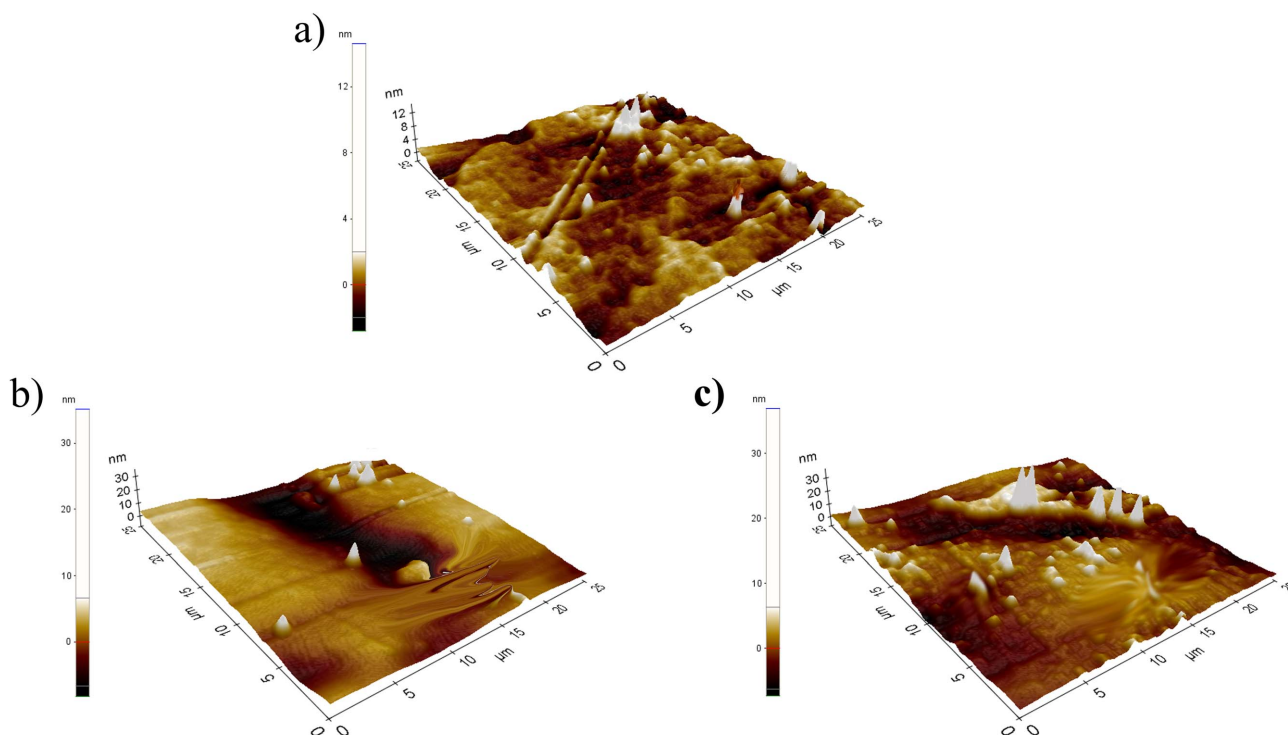


Fig. 4. Results of AFM observation a) Ti<sub>is</sub>, b) Ti<sub>sg</sub>, c) Ti<sub>ald</sub>

### 3.3. Surface roughness analysis by profilometric method

Based on the obtained results it can be concluded that the tested samples were characterized by different surface roughness. The higher value of surface roughness parameter were obtained for the samples in initial state Ti\_is and the mean value was an approximately  $R_a = 0.40 \pm 0.10 \mu\text{m}$ . Deposited zirconia oxide layer leads to decrease surface roughness. The value of the  $R_a$  parameter for both samples group after surface modification were similar and were in the range from 0.08 to 0.10  $\mu\text{m}$ .

TABLE 4

Results of surface roughness measurements

No	Name	$R_a$ [ $\mu\text{m}$ ]
1	Ti_is	$0.40 \pm 0.10$
2	Ti_sg	$0.10 \pm 0.03$
3	Ti_ald	$0.08 \pm 0.01$

### 3.4. Contact angle measurements and Surface Free Energy Calculation

The obtained results of wetting angle measurements and Surface Free Energy components are presented in Table 5 and the examples diagrams of changed value of contact angle in time and drops dripped on the surface of the tested samples are showed in Figure 5. The results for the first samples group 1<sup>st</sup> (Ti\_is) points to hydrophilic character of the surface – the value of the contact angle was less than  $90^\circ$  and was an approximately  $\theta = 79.4 \pm 8^\circ$ . The surface modification by sol-gel method and ALD method effects in the changed chemical character of the surface to hydrophobic. The higher value of wetting angle was obtained for the 3<sup>rd</sup> samples group Ti\_ald and the average value was  $\theta = 115 \pm 11^\circ$ . Based on the obtained results in comparison with the surface roughness measurements and literature data [22-24] it can be concluded, that for the samples characterized by the lower value of the  $R_a$  parameter, the higher value of contact angle can be obtained. The hydrophobic character of the surface are more favorable phenomenon for the decreased bacterial adhesion to the surface of the implants. The value of Surface Free Energy for all tested samples were similar and were in the range of approximately 32-34  $\text{mJ}/\text{m}^2$  and the higher value of apolar components compared to the polar one. Based on this it can be

TABLE 5

Results of contact angle measurements and surface free energy calculation

No	Name	Measure liquid, [°]		Surface Free Energy, [ $\text{mJ}/\text{m}^2$ ]		
		Distilled water	Diiodomethane	$\gamma_s$	$\gamma_d^s$	$\gamma_p^s$
1	Ti_is	$79.4 \pm 8$	$49.8 \pm 7$	32.8	26.6	9.2
2	Ti_sg	$104.6 \pm 11$	$45.4 \pm 9$	31.5	19.8	6.2
3	Ti_ald	$115 \pm 10$	$44.2 \pm 10$	33.9	17.2	4.3

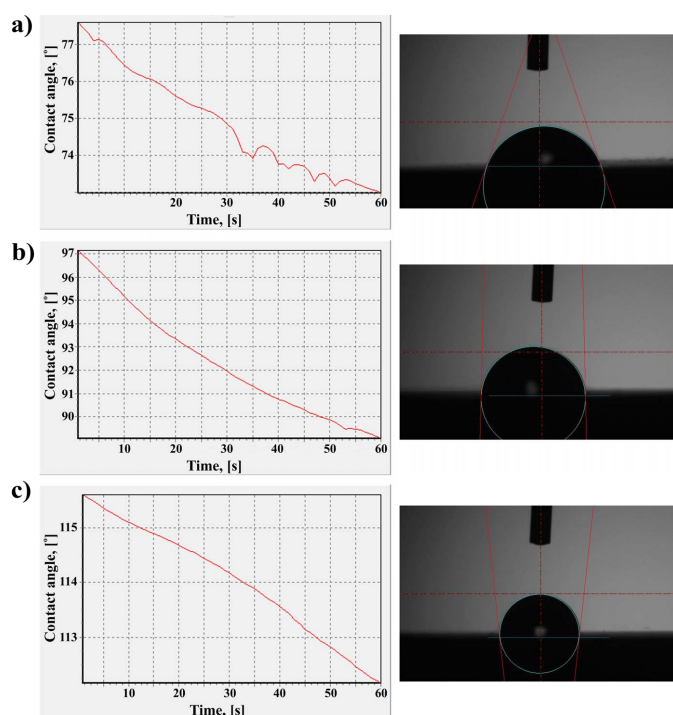


Fig. 5. Examples diagrams of changed value of contact angle in time and drops dripped on the surface of the tested samples a) Ti\_is, b) Ti\_sg, c) Ti\_ald

concluded, that all tested samples exhibit a greater affinity to dispersive groups of SFE that to polar one.

### 3.5. Potentiodynamic testes

The results of the pitting corrosion test in the form of anodic polarization curves for all tested samples are showed in Figure 6 and the values of characteristic parameters of pitting corrosion resistance are presented in Table 6. For the samples in initial state Ti\_is and after surface modification by ALD method Ti\_ald the progress of the curves was typical for the samples with high corrosion resistance – no hysteresis loop were obtained. For both samples group the existence of transpassivation potential has been stated. The higher value of transpassivation potential were obtained for the samples with  $\text{ZrO}_2$  deposited by ALD method Ti\_ald and the mean value was  $E_{tr} = +2500 \pm 102 \text{ mV}$ . The value of transpassivation potential in case of the samples after mechanical treatment was lower and was equal to  $E_{tr} = +1800 \pm 52 \text{ mV}$ . For the samples modified by sol-gel method the progress of anodic curves presents full resistance to pitting corrosion and the polarization potential extends up to the range of  $E = +4000 \text{ mV}$ . The higher value of corrosion resistance were measured for the samples with  $\text{ZrO}_2$  layer deposited by ALD method and the average value was  $E_{corr} = 84 \pm 14 \text{ mV}$ . The values obtained for the other samples were similar and were in the range from – 182 mV for Ti\_is to 142 mV for Ti\_sg.  $\text{ZrO}_2$  coatings, regardless of surface modification method leads to increased value of polarization resistance  $R_p$  and the mean value for the Ti\_sg samples group was  $1.14 \pm 0.15 \Omega/\text{cm}^2$  and for Ti\_ald  $1.27 \pm 0.22 \Omega/\text{cm}^2$ .

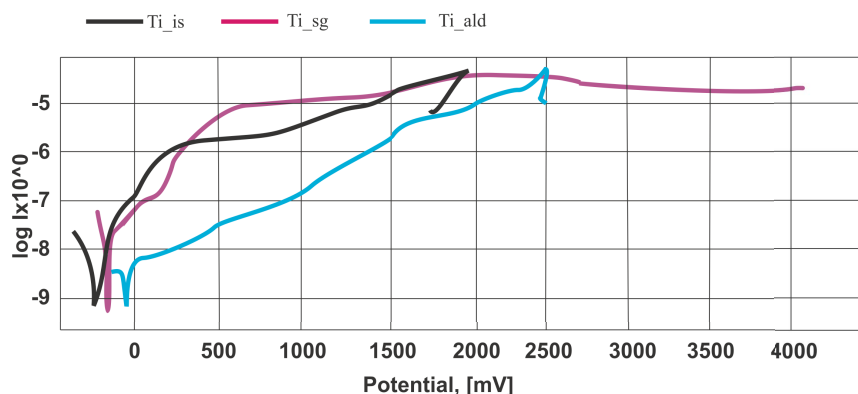


Fig. 6. Results of pitting corrosion test

TABLE 6

Results of pitting corrosion test

No	Name	$E_{corr}$ [mV]	$E_{tr}$ [mV]	$R_p$ [ $\Omega/cm^2$ ]
1	Ti_is	$-182 \pm 21$	$+1800 \pm 52$	$0.75 \pm 0.20$
2	Ti_sg	$-142 \pm 18$	—	$1.14 \pm 0.15$
3	Ti_ald	$-84 \pm 14$	$+2500 \pm 102$	$1.27 \pm 0.22$

### 3.6. Electrochemical Impedance Spectroscopy test

The results of EIS test in the form of impedance spectra (Nyquist diagram and Bode diagram) for tested samples are showed in Figure 7. Based on the equivalent electrical system (Fig. 8) of corrosive systems: tested samples with different surface condition – Ringer’s solution, the parameters of electrical components of the replacement circuit were determined and are presented in Table 7. It was found that for all tested samples, the best fit of the model spectra was provided by equivalent circuits composed of two parallel electric elements representing capaci-

tive or constants CPE of border combined with resistance transitions and resistance  $R$  characteristic for double layer: compact internal and porous external, where:

- $R_s$  – resistance of Ringer solution (electrolyte) recorded at high frequencies,
- $R_{pore}$  – resistance of electrolyte in porous phase,
- $R_{ct}$  – resistance of deposited coating; electric charge transfer resistance at boundary of phases: Ti6Al7Nb alloy – surface layer – electrolyte,
- $CPE_{pore}$  – capacity of the porous surface,
- $CPE_{dl}$  – capacity of deposited coating.

The Nyquist diagram (Fig. 7b) for all tested samples presented fragments of semicircles, which is a characteristic for the thin layer (deposited by the surface modification method or spontaneous formed on the surface in effect contact with the oxygen). The progress of the presented semi-circles were deformed in different degree which can be associated with the near relation between the components of the imaginary impedance  $Z''$  and the real one  $Z'$ . The biggest radius of semicircle was obtained for the samples with zirconia oxide layer deposited by ALD method

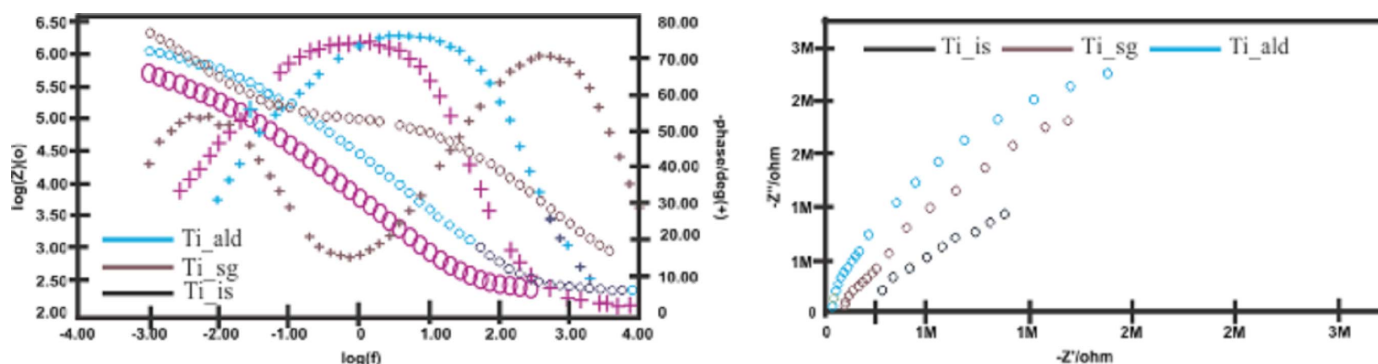


Fig. 7. Results of EIS test

TABLE 7

Results of EIS test

No.	Name	$E_{oper}$ [mV]	$R_s$ [ $k\Omega cm^2$ ]	$R_{pore}$ [ $k\Omega cm^2$ ]	$CPE_{pore}$ [mV]		$R_{cr}$ [ $k\Omega cm^2$ ]	$CPE_{pore}$ [mV]	
					$Y_s$ [ $k\Omega cm^{-m} s^{-n}$ ]	$n$		$Y_s$ [ $k\Omega cm^{-m} s^{-n}$ ]	$n$
1.	Ti_is	-152	37	350	$0.7992E-5$	0.8	$2318 \pm 420$	$0.5432E-5$	0.8
2.	Ti_sg	-152	39	523	$0.7235E-6$	0.8	$4520 \pm 352$	$0.6247E-6$	0.9
3.	Ti_ald	-152	38	592	$0.7589E-6$	0.9	$6250 \pm 324$	$0.8793E-5$	0.9

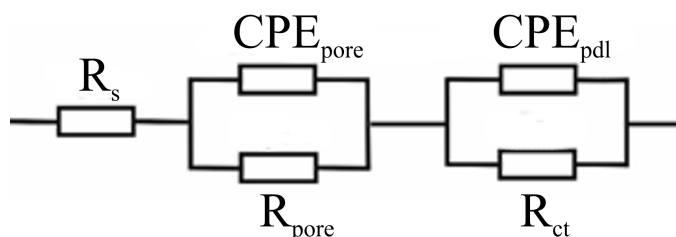


Fig. 8. Equivalent electrical system

Ti<sub>ald</sub>, which indicates to the best corrosion characteristic in tested group. The maximum value of phase displacement at a broad range of frequencies presented in Bode diagram (Fig. 7a) for all tested samples group were similar and were in the range of approximately  $\Theta = 70^\circ$ - $80^\circ$ . Additionally, for the samples in initial state Ti<sub>is</sub> and both with ZrO<sub>2</sub> layer, the inclinations  $\log|Z|$  at the whole scope of frequency change are close to  $-1$ , which indicates the capacitive character of porous layer. The higher value of  $R_{ct}$  parameter were obtained for the Ti<sub>ald</sub> samples group and the mean value was  $R_{ct} = 6250 \pm 324 \text{ k}\Omega\text{cm}^2$ .

#### 4. Conclusion

The correct selection of physicochemical properties is an important issue in the process of adjusting the functionality of biomedical materials used in surgery, orthopedics and dentistry and has a direct impact on the final quality of medical devices. The most important of many physicochemical properties determining the usefulness of a material is its corrosion resistance, wettability and roughness, which are closely related to physical phenomena occurring on its surface.

On the basis of the research results obtained, it was found that [4,22,23]:

1. The type of surface modification method affects the physicochemical properties, including corrosion resistance of the tested material. The samples from ZrO<sub>2</sub> layers applied with the atomic layer deposition (ALD) method are characterized by an optimal set of properties on the implants in comparison to sol-gel method.
2. Moreover the lower values of roughness parameters influence the change of chemical character of the samples to hydrophobic, and better corrosion resistance were obtained for this method.
3. Reduced development of surface topography is conducive to the reduction of bacterial adhesion by reducing the space in which they could be located.

To sum up, the application of ALD method improves anti-corrosion properties. Reduction of surface roughness contributes to slower solution due to corrosive processes. Smooth surface does not generate conditions conducive to aggressive influence of electrolyte (Ringer's solution).

#### REFERENCES

- [1] J.C.B. Alcázar, R.M.J. Lemos, M.C.M. Conde, L.A. Chisini, M.M.S. Salas, B.S. Noremborg, F.V. Motta da, F.F. Demarco, S.B.C. Tarquinio, N.L.V. Carreño, *Prog Org Coat.* **130**, 206-213 (2019).
- [2] O. Bialas, J. Żmudzki, *J. Achiev. Mater. Manuf. Eng* **92**, 29-35 (2019).
- [3] T. Burakowski, *Inżynieria powierzchni metali: podstawy, urządzenia, technologie*, Wydawnictwo Naukowo-Techniczne, Warszawa (1995).
- [4] M. Catauro, F. Barrino, M. Bononi, E. Colombini, R. Giovanardi, P. Veronesi, E. Tranquillo, *Coatings* **9**, 200 (2019), <https://doi.org/10.3390/coatings9030200>.
- [5] R.G. Craig, J.M. Powers, R.L. Sakaguchi, H. Limanowska-Shaw, J.G. Shaw, E. Andrzejewska, *Materiały stomatologiczne*, Elsevier Urban & Partner, Wrocław 127-141 (2008).
- [6] D. S. Juan, Y. Wang, F. Chen, Yu X. Quan, Y. Fa Zhang, *T. Nonferr. Metal. Soc.* **23**, 3027-3032 (2013).
- [7] J. Frostevarg, R. Olsson, J. Powell, A. Palmquist, R. Brånemark, *Appl. Surf. Sci.* **485**, 158-169 (2019).
- [8] W. He, X. Yin, L. Xie, Z. Liu, J. Li, S. Zou, J. Chen, *J. Mater. Sci-Mater. M.* **30** (2019).
- [9] A. Liber-Kneć, S.D. Łagan, *Ćwiczenia laboratoryjne z biomateriałów: pomoc dydaktyczna*, Politechnika Krakowska, Kraków (2011).
- [10] M. Krzywicka, J. Grudziński, *Motrol.* **16** (1), 49-54 (2014).
- [11] J. Marciniak, *Biomateriały*, Wydawnictwo Politechniki Śląskiej, Gliwice, 178-324 (2002).
- [12] J. Marciniak, W. Chrzanowski, A. Kajzer, *Gwoździowanie śródszpikowe w osteosyn-tezie*, Wydawnictwo Politechniki Śląskiej, Gliwice, 89-188 (2006).
- [13] J. Marciniak, M. Kaczmarek, A. Ziębowicz, *Biomateriały w stomatologii*, Wydawnictwo Politechniki Śląskiej, Gliwice, 121-185 (2008).
- [14] A. Miklaszewski, M. Jurczyk, *Weld. Tech. Rev.* **83**, 65-69 (2011).
- [15] C.E. Misch, *Contemporary implant dentistry*, Mosby Elsevier, St. Louis (2008).
- [16] B.E., Pippenger, M. Rottmar, B.S. Kopf, S. Stübinger, F.H. Dalla Torre, S. Berner, Maniura-Weber, *Clin. Oral. Implan. Res.* **30**, 99-110 (2019).
- [17] W. Walke, Z. Paszenda, P. Karasiński, J. Marciniak, *Arch. Mater. Sci. Eng.* **55**, 78-84 (2012).
- [18] [https://www.who.int/gho/mortality\\_burden\\_disease/life\\_tables/situation\\_trends\\_life\\_expectancy/en/](https://www.who.int/gho/mortality_burden_disease/life_tables/situation_trends_life_expectancy/en/)
- [19] D. Buddy Rathner, *Biomaterials science: an introduction to materials in medicine*, Elsevier Academic Press, Amsterdam (2004).
- [20] R.L. Williams, *Surface modification of biomaterials: methods, analysis and applications*, Woodhead Pub, Philadelphia (2011).
- [21] PN – EN ISO 5832-11.
- [22] A. Ziębowicz, A. Woźniak, B. Ziębowicz, M. Adamiak, P. Boryło, *Arch. Mater. Sci. Eng.* **89** (1), 20-26 (2018).
- [23] A. Ziębowicz, A. Woźniak, B. Ziębowicz, *Springer*, 349-357 (2017).
- [24] B. Ziębowicz, A. Woźniak, A. Ziębowicz, A. Ziemińska-Buczyńska, *J. Achiev. Mater. Manuf. Eng.* **93**, 32-40 (2019).